International Journal of Automotive Technology, Vol. 18, No. 3, pp. 463−472 (2017)
DOI 10.1007/s12239−017−0046−0

pISSN 1229−9138/ eISSN 1976−3832

LUMPED MASS-SPRING MODEL CONSTRUCTION FOR CRASH ANALYSIS USING FULL FRONTAL IMPACT TEST DATA

Jae Moon Lim*

Department of Mechanical Engineering Design, Daeduk College, Daejeon 34111, Korea

(Received 30 April 2015; Revised 23 July 2016; Accepted 7 December 2016)

ABSTRACT−Lumped Mass-Spring (LMS) model is simple but very effective for the design study of vehicle crashworthiness and occupant safety. To construct the LMS model, the SISAME software and the NHTSA test data were used. Using the SISAME, the weights of mass elements and the load-paths of spring elements were optimally and directly extracted from the test data. Among the various types of spring, the segmented inelastic type of spring was effective for the vehicle crash analysis. In this study, to obtain the occupant injuries such as HIC_{15} and 3 ms Chest g's, the LMS model containing the occupant model consisted of the head, chest and pelvis was developed and validated. The modeling for the chest deflection and neck injuries was not considered in this study because of the modeling difficulties and the limitation of the SISAME software. The simulation results of occupants showed good agreements with the test results. The modeling idea for the occupant was simple but very effective.

KEY WORDS : Lumped mass-spring model, SISAME, Frontal impact, NCAP, HIC_{15}, Chest g's

1. INTRODUCTION

In the automotive industry, crashworthiness connotes a measure of the vehicle's structural ability to plastically deform and yet maintain a sufficient survival space for its occupants in crashes involving reasonable deceleration loads. The primary aim of the crashworthiness design process is to secure dummy response results that measure below or at acceptable injury risk values. Vehicle crashworthiness and occupant safety remain among the most important and challenging design considerations in the automotive industry (Du Bois *et al*., 2004).

The injury criteria specified in the regulations like Federal Motor Vehicle Safety Standards (FMVSS) No. 208 for full frontal impact test must be met (NHTSA, 2008a). The New Car Assessment Program (NCAP) encourages that the automotive makers shall launch the safer cars into the markets (MLIT, 2012; NHTSA, 2008b). The injury criteria for rating specified in the NCAP are more challenging than the regulations.

Crashworthiness evaluation is ascertained by a combination of tests and analytical methods. Crashworthiness should be assessed by laboratory tests from components to full-scale vehicles. However, testing is both time consuming and expensive. With rapid advancement in digital technology and CAE methodology, the simulation has become an essential and useful tool in the design stage (Du Bois *et al*., 2004; Zuo *et al*., 2016).

**Corresponding author.* e-mail: jmlim@ddc.ac.kr

As the cost-effective alternatives to full-scale vehicle tests, finite element analysis (FEA) has been widely adopted in the vehicle development process (Chen *et al*., 2015; Du Bois *et al*., 2004; Nguyen *et al*., 2015a, 2015b). However, simulations using FEA are still time consuming and expensive because of requiring powerful hardware and software.

Mathematical models can provide quick assessment of various design concepts and explore new design directions (Du Bois *et al*., 2004). Kamal (1970) developed the Lumped Mass-Spring (LMS) model consisted of three rigid masses and eight nonlinear springs for the analysis of vehicle frontal impact. The spring parameters (crush characteristics) of Kamal's model were determined experimentally in a vehicle static crusher (Kamal, 1970).

Marzbanrad and Pahlavani (2011) suggested a system identification algorithm for vehicle lumped parameter model with linear spring and damper in crash analysis.

Pawlus *et al*. (2011a, 2011b, 2014) presented various research results related to the lumped parameter mathematical models using the vehicle to pole collision test results of Ford Fiesta 1987 model. They showed that Maxwell model provide more satisfactory results than Kelvin model under the vehicle-to-pole collision circumstance. Pawlus *et al*. (2011c) showed that the elasto-plastic loading and unloading process of springs play the important role for the accuracy of results. But they did not consider the reloading process of the spring.

This study proposes the LMS modeling method for obtaining the occupant's injuries as well as crash pulse. The

weights of mass elements and the load-paths of spring elements constructing the LMS model are directly and optimally extracted from the full-scale vehicle crash data. For this purpose, the SISAME software was used for the LMS model construction (Mentzer *et al*., 1992; Mentzer, 2007). The SISAME software was originally developed for the National Highway Traffic Safety Administration (NHTSA) (Mentzer *et al*., 1992; Mentzer, 2007). The SISAME software and full-scale vehicle crash test data are publicly available in NHTSA website (NHTSA, 2016a, 2016b).

2. LUMPED MASS-SPRING MODEL

2.1. SISAME Model

The SISAME (Structural Impact Simulation And Model Extraction) is a general purpose tool for extracting and simulating one-dimensional nonlinear lumped parameter structural models. A simple model configuration of a vehicle-to-barrier test is shown in Figure 1 (Mentzer, 2007). To construct spring-mass model suggested in Figure 1 using the SISAME, accelerations at the locations of B-pillar, engine and disc brake caliper, and forces from the barrier loadcells need to be obtained from full-scale crash test data. Users can add masses and springs in the model. To add the mass elements in the model, the accelerations at the location of mass elements need to be measured during the crash test. The locations of accelerometers are shown in Figure 2.

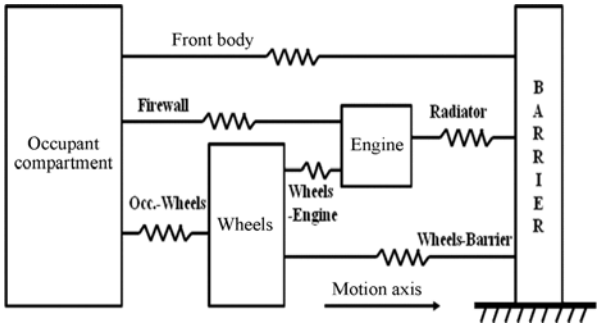

Figure 1. Simple vehicle model configuration.

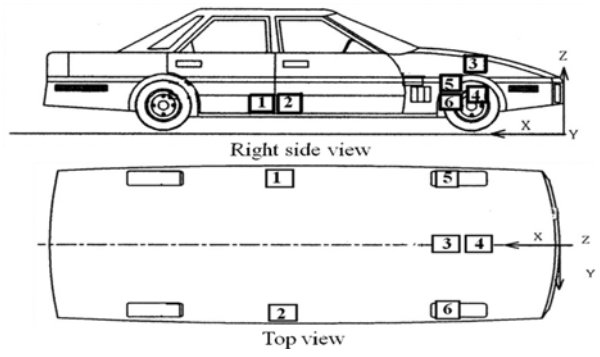

Figure 2. Vehicle accelerometer locations.

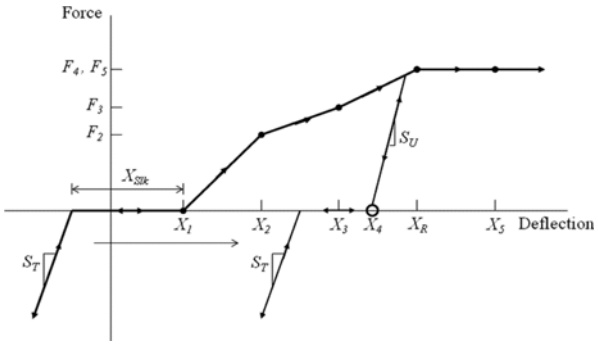

Figure 3. Force-deflection of segmented inelastic spring.

The procedures to construct the simulation model using the SISAME consist of two stages. In the first stage, the weights of the mass elements are extracted using accelerations and wall forces from the test data. In the second stage, the load-paths of spring elements are extracted using the weights of mass elements obtained from the first stage and accelerations from the test data. The weights of mass elements and the load-paths of spring elements are optimally extracted that the motions of mass elements satisfy the accelerations and forces of the test data.

The SISAME provides five types of elastic (path-independent) springs and three types of inelastic (path-dependent) springs. In this study, the segmented inelastic type of spring is used, as represented in Figure 3. This spring loads up the segmented compression boundary with increasing (compressive) deflections, unloads along a straight line with unloading slope S_U to zero force, maintains zero force for a deflection equal to the slack, X_{Slk}, and then loads in tension along a line with slope S_T. Subsequent loading-unloading remains on this unloading/tension path until loading again reaches the compression boundary and inelastic deformation continues, moving the unloading point with it. This spring type is intended to capture the static deformation behavior of an idealized compound structure under compressive impact loading. Dynamic effects are typically applied to the springs to model strain rate and dynamic magnification phenomena. The parameters of S_U, S_T, X_{Slk} and dynamic effects are obtained during the load-paths extraction process. The setup of the parameters of S_U, S_T, X_{Slk} and dynamic effects may affect the stability and accuracy of the simulation results as well as the extraction process of the load-paths of springs.

2.2. Lumped Mass-spring Model with Occupants

The Lumped Mass-Spring (LMS) model developed in this study is represented in Figure 4. The upper parts of dummies are considered to obtain the injuries of occupants. The lower parts of dummies are excluded because the injuries like the femur loads are difficult to obtain at this time, using the SISAME. The dummy on the driver seat is

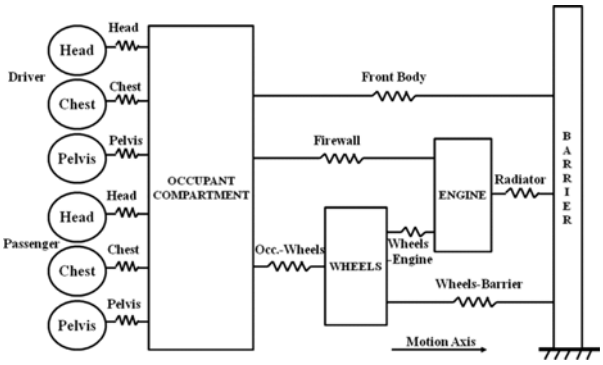

Figure 4. Simple vehicle model configuration with occupants.

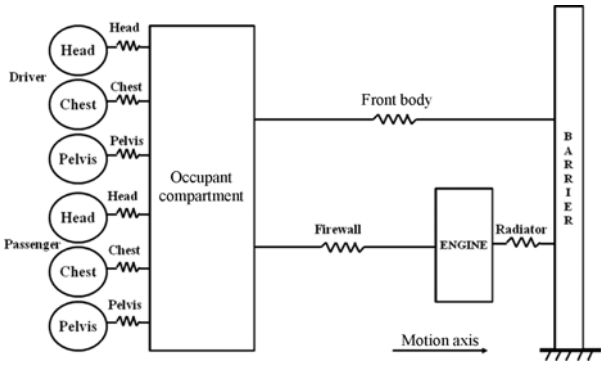

Figure 5. Modified simple vehicle model configuration with occupants.

the 50th percentile male Hybrid III dummy. The dummy on the right front passenger seat will be the 50th percentile male Hybrid III dummy or the 5th percentile female Hybrid III dummy under the condition of test method. To enhance the safety of smaller occupants, the dummy on the right front position uses the 5th percentile female Hybrid III dummy for the full frontal impact test in the KNCAP and US-NCAP (Lee and Lim, 2014; MLIT, 2012; NHTSA, 2008b).

3. MODEL CONSTRUCTION

In this study, the US-NCAP frontal impact test data were used to construct the LMS model (NHTSA, 2016a, 2016b). The website of NHTSA contains the vast and various full-size crash test data since 1978 (NHTSA, 2016b). The brief specifications of tested vehicles are represented in Table 1 (Janovicz and Fischer, 2011, 2012, 2014; Walsh and Dutton, 2014). The full frontal barrier impact test was conducted at the speed of 56 km/h. Four midsize cars from two different automakers were selected. Since the accelerometers at the disc brake (position 5 and 6 shown in the Figure 6) were not attached and measured for the vehicles tested after MY2013 (NHTSA, 2016b), the characteristics of constructed models due to without the wheels mass and related springs need to be compared. This configuration is shown in Figure 5. Therefore, the configuration represented in Figure 4 is used for the vehicles tested before MY2013 and the configuration represented in Figure 5 is used for the vehicles tested after MY2013.

Table 1. Specifications of vehicles.

Vehicle	Camry12	Camry14	Sonata11	Sonata15
Model year	2012	2014	2011	2015
Type	4-door sedan	4-door sedan	4-door sedan	4-door sedan
Weight (kg)	1662	1664	1670	1712
Engine Displ. (l)	2.5	2.5	2.4	2.4

Table 2. Weights of dummy parts.

Dummy	Head	Chest	Pelvis
Hybrid III male	4.54 kg	17.19 kg	23.04 kg
Hybrid III female	3.74 kg	12.03 kg	13.26 kg

Table 3. Weights of vehicle parts.

Vehicle	Occupant Compartment	Engine	Wheels
Camry12	1,308.2 kg	200.0 kg	80 kg
Camry14	1,390.2 kg	200.0 kg	-
Sonata11	1,316.2 kg	200.0 kg	80 kg
Sonata15	1,357.7 kg	280.5 kg	-

The weights of mass elements except dummies were extracted in the first stage using the weight extraction model consisted of the barrier force from load cells and the accelerations from B-pillar, engine and disk brakes. The weights of dummy parts were obtained from HUMANETICS (2016). In the process of extracting the weights of vehicle parts, the weights of dummy parts were added respectively in the weight extraction model. Accelerations and barrier forces of the parts were averaged respectively before the model extraction processes. Since the SISAME model is one-dimensional structures and one mass element needs one signal of the part. Averaging the signals from the accelerometers and loadcells provides the reasonable results during the extraction processes and the simulations runs.

The weight extraction was performed with 60 Hz cutoff frequency since the barrier force is a sum of signals and contains little higher frequency content (Mentzer *et al*., 1992; Mentzer, 2007). The weights of dummy parts and vehicle parts were represented in Table 2 and Table 3.

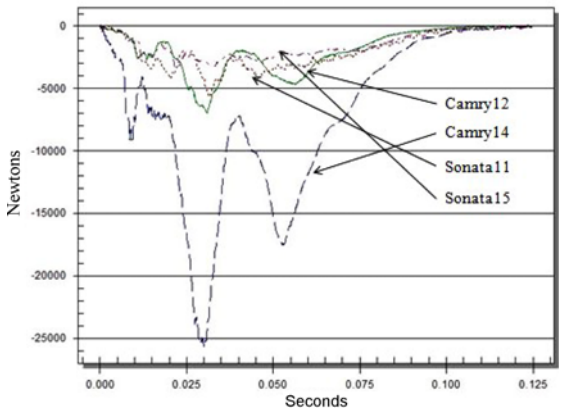

Figure 6. Averaged barrier forces of vehicles.

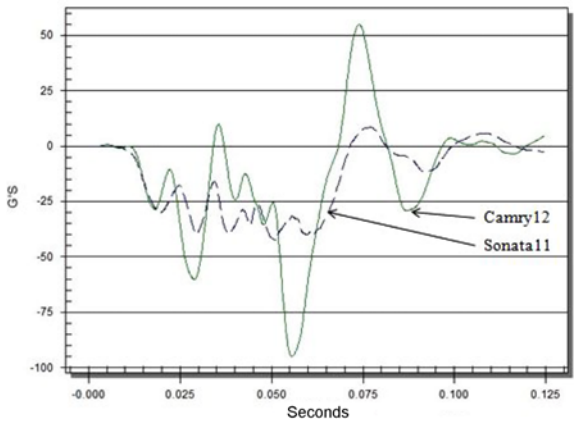

Figure 9. Accelerations at the disc brake.

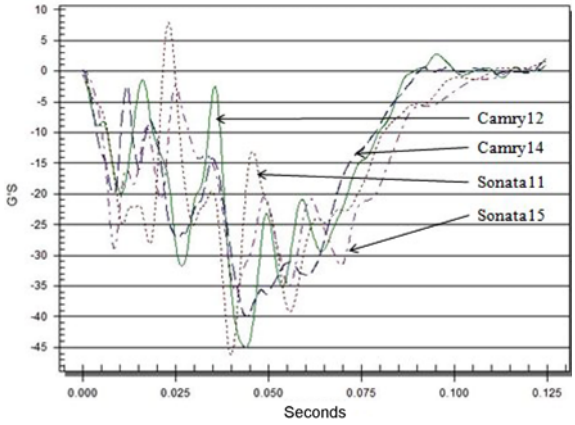

Figure 7. Accelerations at the B-pillar.

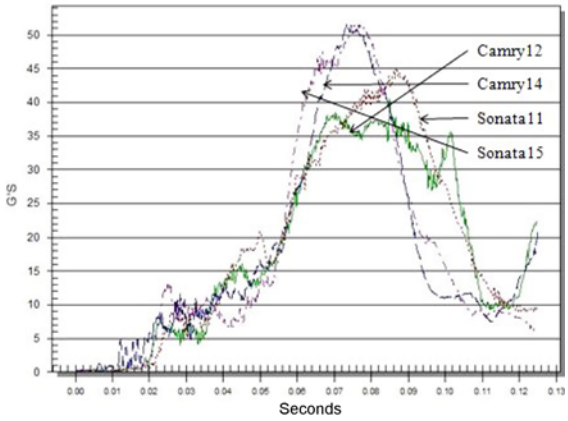

Figure 10. Accelerations at the driver head.

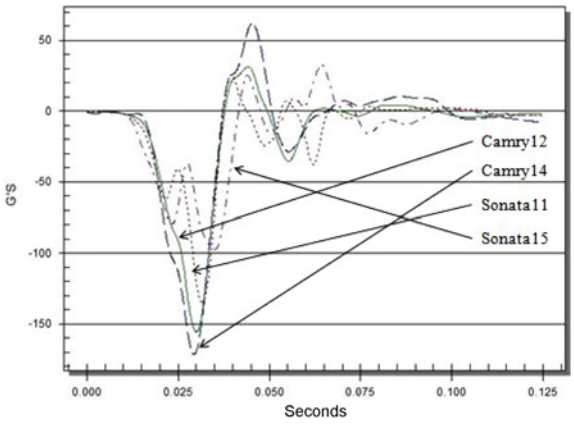

Figure 8. Accelerations at the engine.

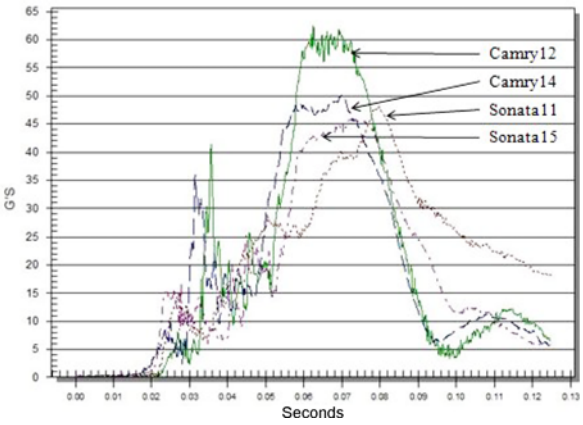

Figure 11. Accelerations at the passenger head.

Barrier forces and accelerations of the tested vehicles for constructing the LMS model are represented in Figures 6 ~ 15. As shown in Figure 6, the barrier force of Camry14 is much greater than those of other vehicles. The type of loadcells might cause the big difference of barrier forces. The loadcells for the Camry14 consisted of 4 rows and 9 columns (Walsh and Dutton, 2014). The loadcells for the Camry12, Sonata11 and Sonata15 consisted of 8 rows and 16 columns (Janovicz and Fischer, 2011, 2012, 2014). As shown in Figure 9, the accelerations at the disc brake locations of the Camry14 and Sonata15 were not measured. Approximated through the extraction process, the extracted weights of body parts could be different from the exact values for the parts.

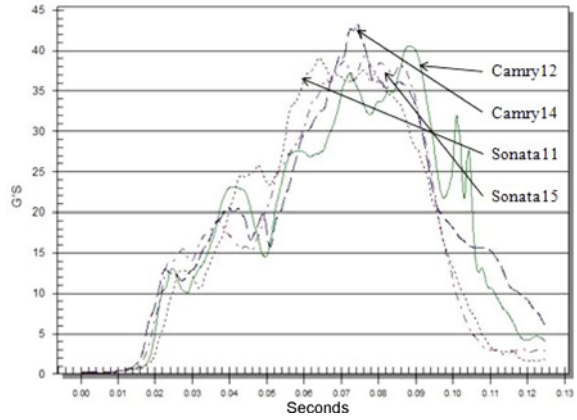

Figure 12. Accelerations at the driver chest.

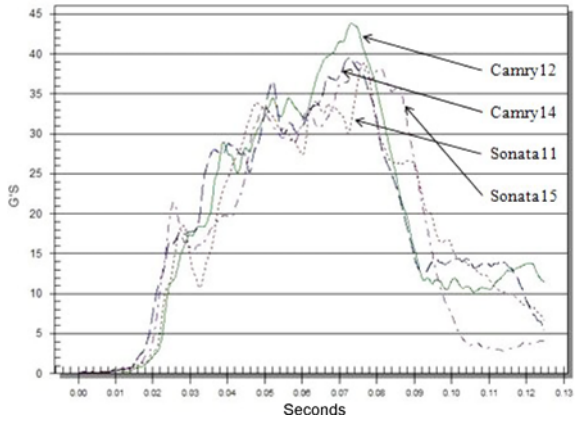

Figure 13. Accelerations at the passenger chest.

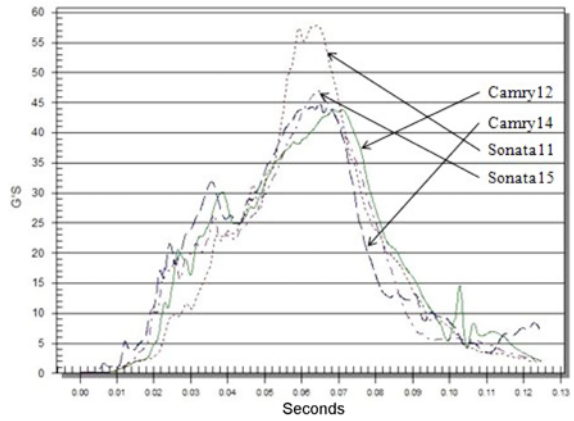

Figure 14. Accelerations at the driver pelvis.

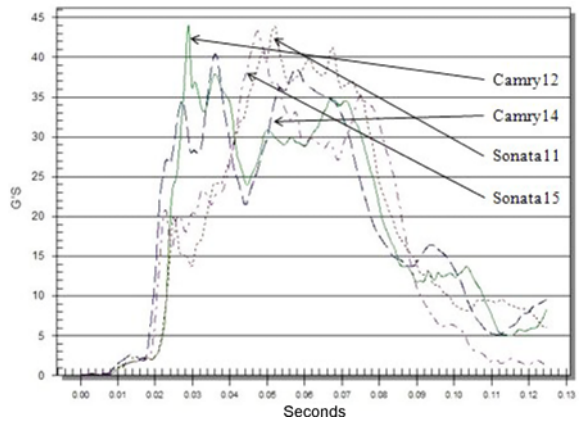

Figure 15. Accelerations at the passenger pelvis.

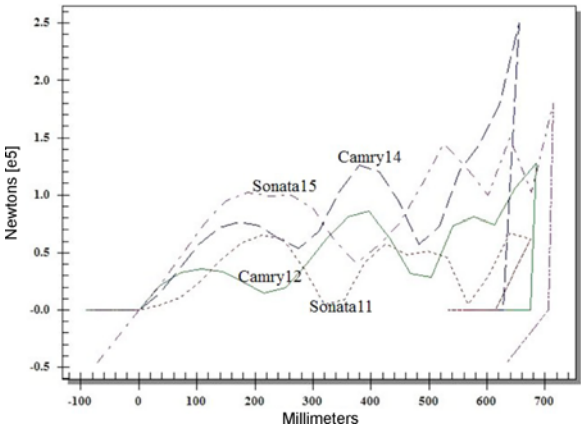

Figure 16. Front body force-deflection curve.

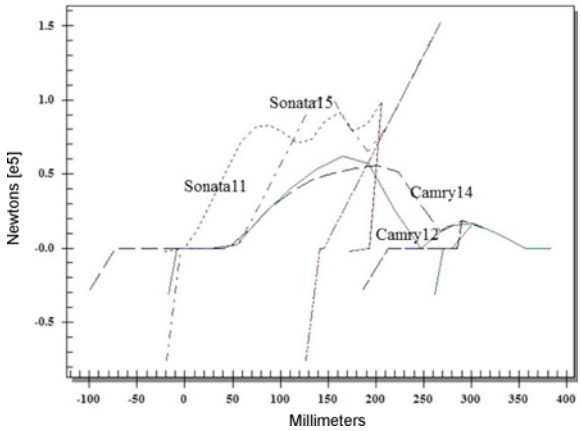

Figure 17. Firewall force-deflection curve.

In the second stage of the model extraction process, the load-paths of all springs were extracted using the weights of mass elements and the accelerations from test data using the load-paths extraction model. The model for Camry12 and Sonata11 represented in Figure 4 obtains twelve load-paths of springs. The model for Camry14 and Sonata15 represented in Figure 5 obtains nine load-paths of springs. The load-paths extraction was performed with the cutoff frequencies of 60 Hz for the car body parts, 1000 Hz for the dummy head, and 180 Hz for the chest and pelvis of dummy. The force-deflection curves for the extracted load-paths of springs are represented in Figures 16 ~ 27.

Finally, the simulation model for the full frontal impact analysis is obtained using the weights of mass elements and

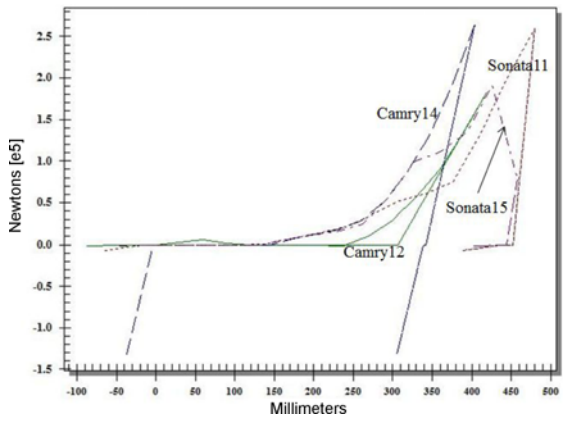

Figure 18. Radiator force-deflection curve.

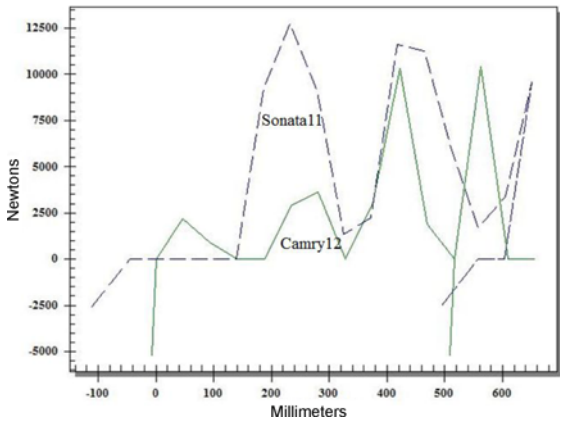

Figure 21. Wheels-Barrier force-deflection curve.

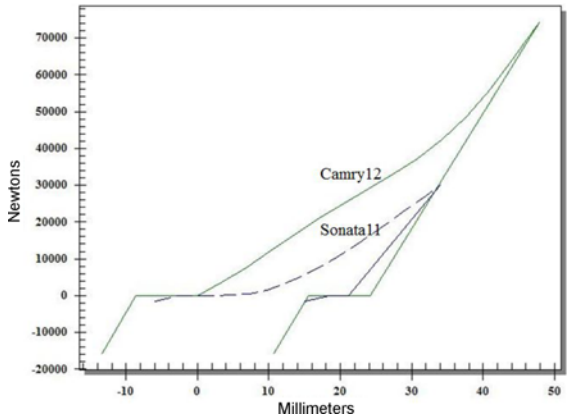

Figure 19. Occ.-Wheels force-deflection curve.

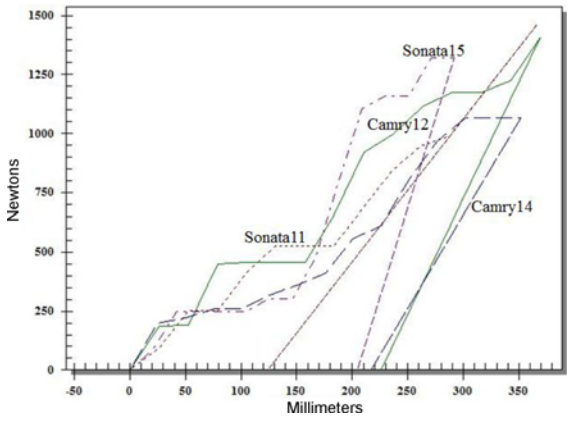

Figure 22. Driver head force-deflection curve.

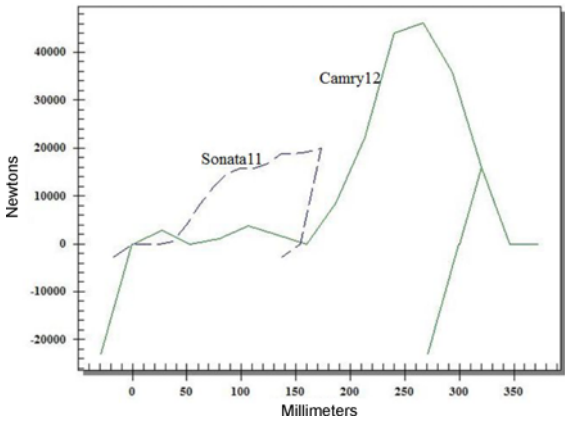

Figure 20. Wheels-Engine force-deflection curve.

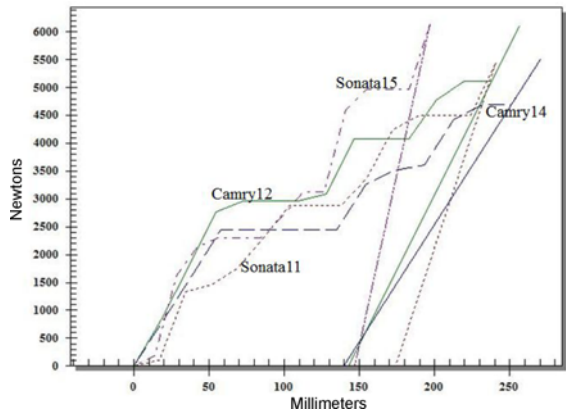

Figure 23. Driver chest force-deflection curve.

the load-paths of spring elements. The accelerations, velocities and displacements of mass elements can be obtained through the simulation runs. The design process using the load-paths of springs can be performed and optimized to reduce the occupant injuries.

4. RESULTS AND DISCUSSIONS

To investigate the effectiveness of the LMS model developed in this study, the accelerations of B-pillar from simulation results are compared with the test results. Also,

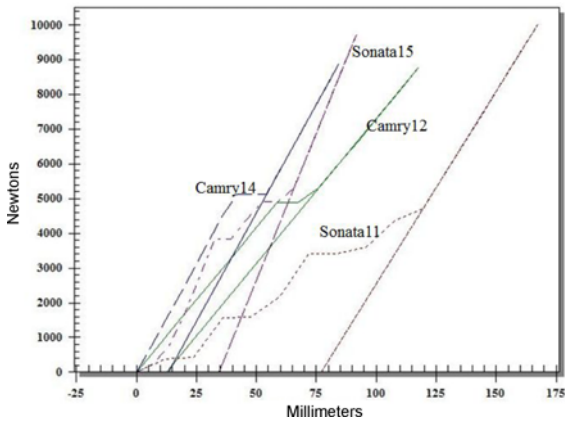

Figure 24. Driver pelvis force-deflection curve.

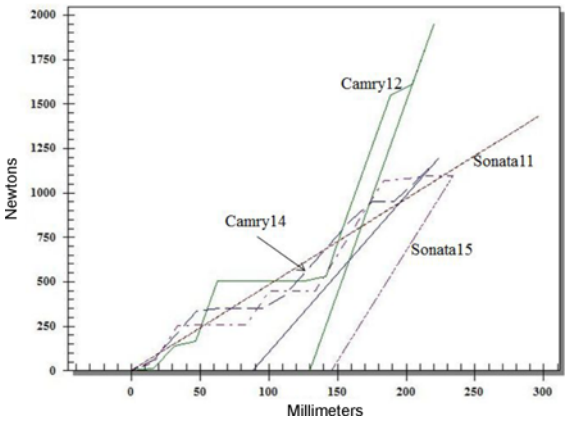

Figure 25. Passenger head force-deflection curve.

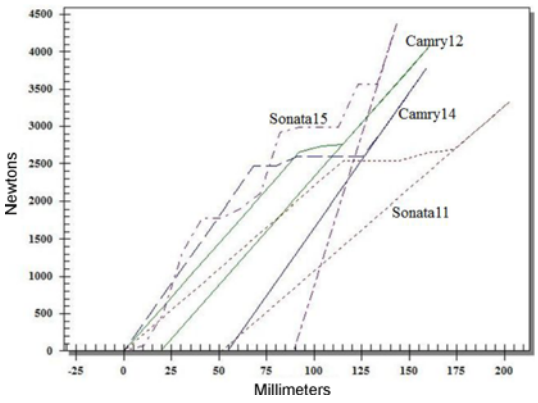

Figure 26. Passenger chest force-deflection curve.

the HIC_{15} and chest g's between tests and simulations are compared. The HIC_{15} is represented in Equation (1) (NHTSA, 2008a). The Chest g's is 3 ms peak acceleration. Though the chest deflection is used for the ratings of chest injury these days in NCAP (MLIT, 2012; NHTSA, 2008b), the chest g's is used for the occupants injury in this study. Since the deflection of rigid mass element for the chest is not possible at this time.

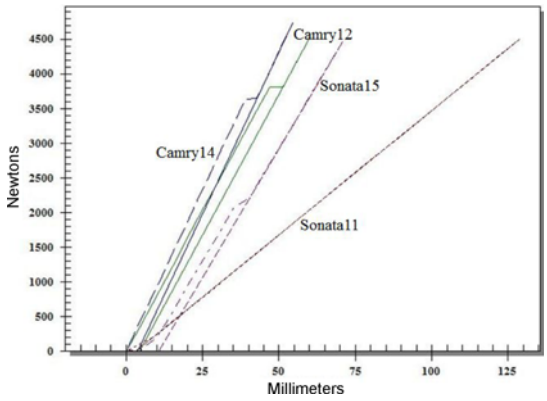

Figure 27. Passenger pelvis force-deflection curve.

$$HIC_{15} = \max\left\{\left[\frac{1}{(t_2 - t_1)}\int_{t_1}^{t_2} a_r dt\right]^{2.5}(t_2 - t_1)\right\} \quad (1)$$

where t_2 and t_1 are any two arbitrary times during the acceleration pulse. The HIC_{15} and chest g's are represented in Tables 4 and 5. The results show good correlation between tests and simulations. The errors are all below 10 %. The LMS model using the test data of vehicle after MY2013 was simpler than the model using the test data of vehicles before MY2013 but the model still provided good results. The accelerations of the driver head for Sonata15 and the accelerations of the passenger chest for Camry14 are represented in Figures 28 and 29, respectively. Since

Table 4. Comparison of test and simulation results for the HIC_{15}.

Vehicle	Driver			Passenger		
	Test	Simula-tions	Error (%)	Test	Simula-tions	Error (%)
Camry12	122	123	0.8	398	388	2.6
Camry14	236	223	5.8	240	243	1.2
Sonata11	173	173	0.0	183	189	3.2
Sonata15	245	229	7.0	197	195	1.0

Table 5. Comparison of test and simulation results for the 3 ms Chest g's.

Vehicle	Driver			Passenger		
	Test	Simula-tions	Error (%)	Test	Simula-tions	Error (%)
Camry12	40.0	37.5	6.7	43.0	41.8	2.9
Camry14	42.2	39.8	6.0	38.5	41.7	7.7
Sonata11	38.0	38.0	0.0	37.0	35.1	5.4
Sonata15	38.0	38.0	0.0	38.0	36.8	3.3

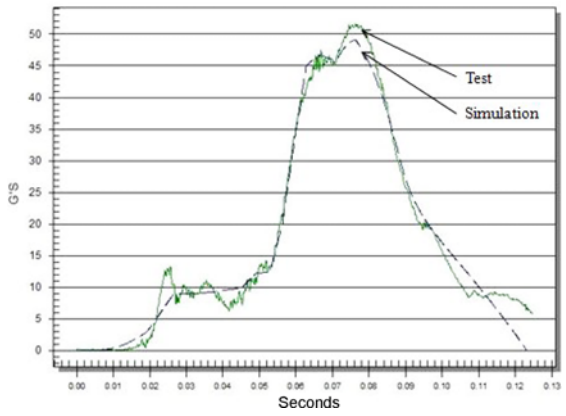

Figure 28. Driver head accelerations of Sonata15.

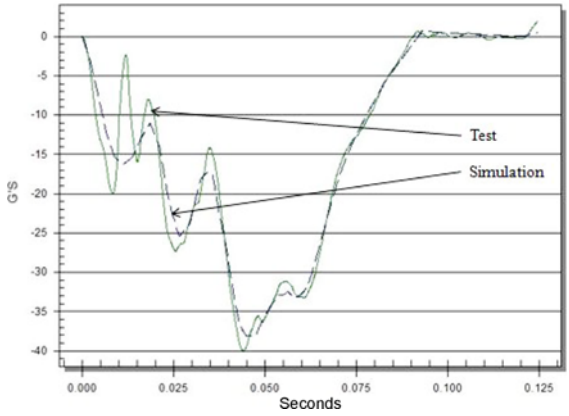

Figure 31. B-pillar accelerations of Camry14.

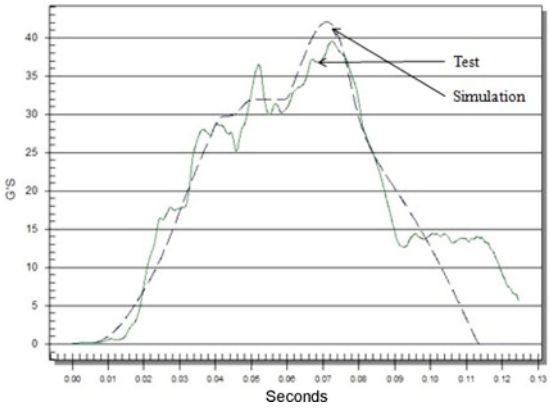

Figure 29. Passenger chest accelerations of Camry14.

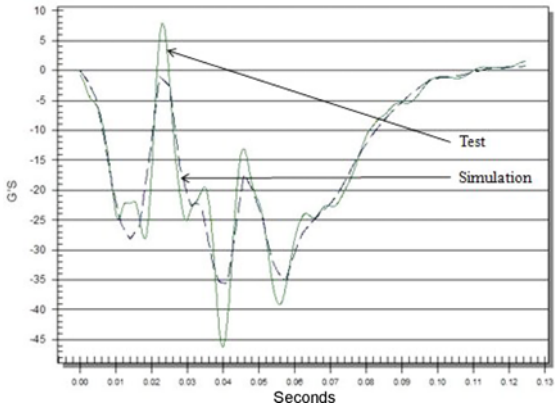

Figure 32. B-pillar accelerations of Sonata11.

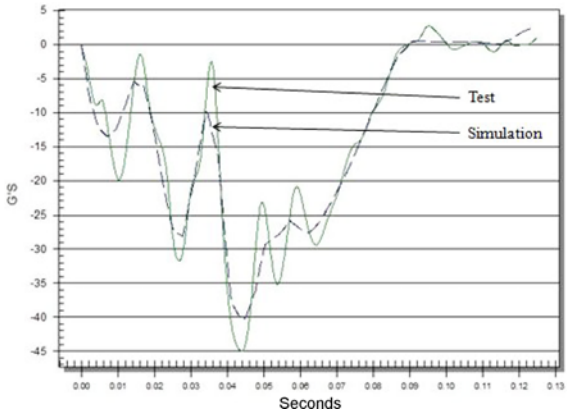

Figure 30. B-pillar accelerations of Camry12.

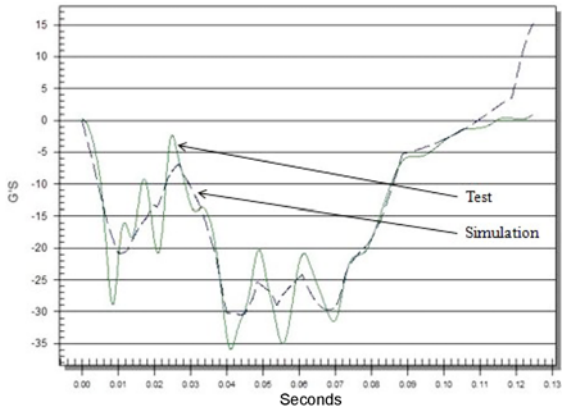

Figure 33. B-pillar accelerations of Sonata15.

their head and chest injuries between test and simulation represent the biggest difference in this study. As shown in Figures 28 and 29, the overall behaviors of the mass elements representing the head and chest agreed well with those of the test vehicles except the differences between the peak values. As represented above, the modeling method developed in this study is simple but very effective for the estimation of occupant behaviors.

In this study, the chest deflection and neck injuries were not considered. In the various NCAP, the chest deflection and neck injuries play the important role of rating the vehicle together with the HIC. It is difficult to construct the model of the chest deflection and neck injuries for the current SISAME software.

The accelerations of B-pillar are represented in Figures 30 ~ 33. The overall behaviors of the simulation models

agreed very well with those of the test vehicles except the differences between the peak values. The accelerations of B-pillar are the essential feature in the design process and can be the design variables to reduce the risk of injuries of occupants under the full frontal impact scenarios (Du Bois *et al*., 2004; Urbina *et al*., 2014).

Through the extraction process for the load-paths of springs, the segmented inelastic type of spring was effective to construct the model. Since the extraction processes for the springs were optimally converged. Also, the results of occupants and B-pillar were stable and accurate. If engineers want to enhance the safety of a vehicle, the improved design for the vehicle structure can be obtained through the design studies of the load-paths of springs.

5. CONCLUSION

To construct the Lumped Mass-Spring model, the SISAME software developed by the NHTSA and the US-NCAP frontal impact test data were used. The test data of four midsize cars of two automakers were selected and processed. Using the SISAME, the weights of mass elements and the load-paths of spring elements were optimally and directly extracted from the test data. Among various types of spring, the segmented inelastic type of spring was very effective for the construction of LMS model.

In this study, the occupant model for the LMS model was developed and validated. The occupant model was consisted of the head, chest and pelvis of the dummies. The lower parts of the occupant were not considered in this study. The simulation results of the head and chest injuries showed good agreement with the test results. The idea was simple but very effective for the estimation of the behaviors for the head and chest of dummies.

The LMS model using the test data after MY2013 was simpler than the model using the test data before MY2013 but the model still provided good results.

In this study, the chest deflection and neck injuries were not considered. It is difficult to construct the model of the chest deflection and neck injuries for the current SISAME software. In the future study, if the modeling difficulties solved, the chest deflection and neck injuries need to be considered.

REFERENCES

Chen, D. Y., Wang, L. M., Wang, C. Z., Yuan, L. K., Zhang, T. Y. and Zhang, Z. Z. (2015). Finite element based improvement of a light truck design to optimize crashworthiness. *Int. J. Automotive Technology* **16**, **1**, 39–49.

Du Bois, P., Chou, C. C., Fileta, B. B., Khalil, T. B., King, A. I., Mahmood, H. F., Mertz, H. J. and Wismans, J. (2004). *Vehicle Crashworthiness and Occupant Protection*. American Iron and Steel Institute. Michigan, USA.

HUMANETICS (2016). http://www.humanetics.com

Janovicz, D. and Fischer, B. (2011). Final Report of New Car Assessment Program Frontal Impact Testing of a 2011 Hyundai Sonata GLS 4-Dr Sedan. NCAP-MGA-2011-060. NHTSA No. UB0501. MGA Research Co., USA.

Janovicz, D. and Fischer, B. (2012). Final Report of New Car Assessment Program Frontal Impact Testing of a 2012 Toyota Camry LE 4-Dr Sedan. NCAP-MGA-2012-027. NHTSA No. YC5100. MGA Research Co., USA.

Janovicz, D. and Fischer, B. (2014). Final Report of New Car Assessment Program Frontal Impact Testing of a 2015 Hyundai Sonata SE 4-Dr Sedan. NCAP-MGA-2015-007. NHTSA No. O20154203. MGA Research Co., USA.

Kamal, M. M. (1970). Analysis and simulation of vehicle to barrier impact. *SAE Paper No*. 700414.

Lee, K. W. and Lim, J. M. (2014). Comparison on rating methods for female dummy in NCAP frontal impact test. *Int. J. Automotive Technology* **15**, **6**, 919–925.

Marzbanrad, J. and Pahlavani, M. (2011). A system identification algorithm for vehicle lumped parameter model in crash analysis. *Int. J. Modeling and Optimization* **1**, **2**, 163–168.

Mentzer, S. G., Radwan, R. A. and Hollowell, W. T. (1992). The SISAME methodology for extraction of optimal lumped parameter structural crash models. *SAE Paper No*. 920358.

Mentzer, S. G. (2007). The SISAME Program: Structural Crash Model Extraction and Simulation. DOT HS Final Report. National Highway Traffic Safety Administration, USA.

MLIT (2012). Provisions on New Car Assessment Program. Public Notice No. 2012-351. Ministry of Land, Infrastructure and Transport, Korea.

Nguyen, P. T. L., Lee, J. Y., Yim, H. J., Lee, S. B. and Heo, S. J. (2015a). Analysis of vehicle structural performance during small-overlap frontal impact. *Int. J. Automotive Technology* **16**, **5**, 799–805.

Nguyen, P. T. L., Lee, J. Y., Yim, H. J., Kim, H. K., Lee, S. B. and Heo, S. J. (2015b). Optimal design of vehicle structure for improving small-overlap rating. *Int. J. Automotive Technology* **16**, **6**, 959–965.

NHTSA (2008a). Occupant Protection. Federal Motor Vehicle Safety Standard (FMVSS). 208. National Highway Traffic Safety Administration, USA.

NHTSA (2008b). Consumer Information; New Car Assessment Program. Docket No. NHTSA-2006-26555. National Highway Traffic Safety Administration, USA.

NHTSA (2016a). SISAME Modeling Project Homepage. http://www-nrd.nhtsa.dot.gov/software/sisame. National Highway Traffic Safety Administration, USA.

NHTSA (2016b). NHTSA Vehicle Crash Test Database. http://www-nrd.nhtsa.dot.gov/database/veh/veh.htm. National Highway Traffic Safety Administration, USA.

Pawlus, W., Karimi, H. R. and Robbersmyr, K. G. (2011a). Development of lumped-parameter mathematical models for a vehicle localized impact. *Int. Mechanical Science and Technology* **25**, **7**, 1737–1747.

Pawlus, W., Karimi, H. R. and Robbersmyr, K. G. (2011b). Application of viscoelastic hybrid models to vehicle crash simulation. *Int. J. Crashworthiness* **16**, **2**, 195–205.

Pawlus, W., Karimi, H. R. and Robbersmyr, K. G. (2011c). Mathematical modeling of a vehicle crash test based on elasto-plastic unloading scenarios of spring-mass models. *Int. J. Advanced Manufacturing Technology* **55**, **1**, 369–378.

Pawlus, W., Karimi, H. R. and Robbersmyr, K. G. (2014). Investigation of vehicle crash modeling techniques: Theory and application. *Int. J. Advanced Manufacturing Technology* **70**, **5**, 965–993.

Urbina, P., Orta, P. and Ahuett-Garza, H. (2014). Crashworthiness design based on a simplified deceleration pulse. *Int. J. Automotive Technology* **15**, **6**, 909–917.

Walsh, V. and Dutton, E. (2014). Final Report of New Car Assessment Program Frontal Impact Testing of a 2014.5 Toyota Camry Four Door Sedan. NCAP-CAL-14-009. NHTSA No. M20145109. Calspan Co., USA.

Zuo, W., Yu, J. and Saitou, K. (2016). Stress sensitivity analysis and optimization of automobile body frame consisting of rectangular tubes. *Int. J. Automotive Technology* **17**, **5**, 843–851.